



# Radiation Transfer Modeling in Electrothermal Chemical (ETC) Ignition

by Klaus Kappen

ARL-CR-506

September 2002

prepared by

Klaus Kappen  
Esterwagnerstraße 19 A  
85635 Höhenkirchen  
GERMANY

under contract

DAAH04-96-C-0086, TCN 01033

## **NOTICES**

### **Disclaimers**

The findings in this report are not to be construed as an official Department of the Army position unless so designated by other authorized documents.

Citation of manufacturer's or trade names does not constitute an official endorsement or approval of the use thereof.

Destroy this report when it is no longer needed. Do not return it to the originator.

# Army Research Laboratory

Aberdeen Proving Ground, MD 21005-5066

---

ARL-CR-506

September 2002

---

## Radiation Transfer Modeling in Electrothermal Chemical (ETC) Ignition

Klaus Kappen

Guest Researcher

prepared by

Klaus Kappen

Esterwagnerstraße 19 A

85635 Höhenkirchen

GERMANY

under contract

DAAH04-96-C-0086, TCN 01033

---

---

## **Abstract**

---

The use of plasma ignition for high-performance guns has been pursued at several levels. As part of the program at the U.S. Army Research Laboratory (ARL), we are attempting to define the role of the broadband electromagnetic radiation that is a key energy component of the plasma discharge. In particular, this effort is developing a radiation transfer model that will be incorporated into the computational fluid dynamics (CFD) model of plasma ignition. This effort will allow more physically realistic characterization of the energy transfer in the plasma and its interaction with the propellant in the models.

This report summarizes the physical background of the radiation transport, and the validation of the different submodules by use of published data will be presented. Current efforts include the coupling of the radiation model to the ARL NSRG2 code for the plasma-propellant interaction simulation. Furthermore, a series of laboratory experiments will be performed to validate the CFD code with the incorporated radiation transport submodel.

---

## **Acknowledgments**

---

The author would like to thank the U.S. Army Research Laboratory (ARL) for funding this Scientific Service Agreement under Contract No. DAAH04-96-C-0086, TCN 01033. Thanks also go to David Mann of the Army Research Office for supporting this contract and to Jack Franklin of Battelle, by whom the contract is transacted. The excellent support and teamwork of Richard Beyer and Mike Nusca of ARL are highly appreciated. Special thanks go to Rose Pesce-Rodriguez, who has done a tremendous job establishing this contract.

INTENTIONALLY LEFT BLANK.

---

## Contents

---

<b>Acknowledgments</b>	<b>iii</b>
<b>List of Figures</b>	<b>vii</b>
<b>List of Tables</b>	<b>vii</b>
<b>1. Introduction</b>	<b>1</b>
<b>2. Physical Background</b>	<b>1</b>
2.1 Equation of State (EOS).....	2
2.2 Absorption Coefficients .....	3
2.3 Method of Partial Characteristics .....	6
2.4 Three-Dimensional (3-D) Radiation Transfer .....	7
<b>3. Validation</b>	<b>7</b>
3.1 Atomic Data .....	7
3.2 Net Emission Coefficients.....	10
<b>4. Radiation Transport in CFD Simulations</b>	<b>11</b>
<b>5. Summary</b>	<b>12</b>
<b>6. References</b>	<b>13</b>
<b>Report Documentation Page</b>	<b>17</b>

INTENTIONALLY LEFT BLANK.

---

## List of Figures

---

Figure 1. Calculated LTE number densities of a polyethylene (C <sub>2</sub> H <sub>4</sub> ) plasma at (a) 1 MPa and (b) 10 MPa. ....	4
Figure 2. Comparison of calculated total effective continuum cross section for NI at 15,000 K. The results of Armstrong et al. [30] have been published by Wilson and Nicolet [25]. ....	9
Figure 3. Emissivities of hydrogen (a) N <sub>e</sub> = 2.9 × 10 <sup>16</sup> cm <sup>-3</sup> and T = 10,850K and (b) N <sub>e</sub> = 9.3 × 10 <sup>16</sup> cm <sup>-3</sup> and T = 13,140 K, compared to experimental data of Wiese et al. [10]. The thin lines are the contribution due to lines and the continuum. The smooth dissolution of the line into the continuum agrees very well with the measurements. ....	10
Figure 4. Net emission coefficients of (a) an isothermal air plasma at different radii and (b) an isothermal SF <sub>6</sub> plasma of radius 0.1 cm, compared to results of Sevastyanenko and Soloukhin [32], Gleizes et al. [33], Liebermann and Lowke [34], and Aubrecht and Gross [35]. All calculations have been performed for atmospheric pressure. ....	11

---

## List of Tables

---

Table 1. Comparison of some calculated oscillator strengths of neutral carbon CI to data of Wiese et al. [29]. ....	8
Table 2. Comparison of some calculated Stark broadened widths (FWHM) for single ionized carbon CII. ....	9

INTENTIONALLY LEFT BLANK.

---

## 1. Introduction

---

The plasma ignition of high-loading densities has been investigated for many years and in various gun calibers. The advantages of these adjustable igniters (e.g., a temperature compensation effect) have been demonstrated in many firings, and the interaction of the plasma with the propellant has been the focus of many open-air and closed-vessel experiments. Yet, not all of the physical and chemical effects of the plasma-propellant interaction (PPI) are understood in adequate detail.

Many experimental investigations have indicated that the energy transfer by plasma radiation is an important effect for a fast ignition of the propellant as well as an enhanced mass conversion [1–4, 5]. Whether or not it dominates all other energy transport mechanisms from the plasma source to the propellant will depend strongly on the ignition concept (e.g., Plasma-Jet, Current Injection) and its parameters (like geometry, pulse duration, pressure levels, etc.). Independent of the PPI effects, radiation is the dominant effect of energy transport within the hot plasma. It has been known for many years that the ohmic heating of the plasma (by the electrical energy release) is mainly balanced by radiation. Therefore, radiation transport has to be taken into account when solving the energy balance equation in any electrothermal chemical (ETC) computational fluid dynamics (CFD) calculations and when studying and simulating PPI effects.

In this report, the status of a new radiation transport model will be described, which will be coupled to the ARL CFD code NSRG2 for a more physically realistic description of plasma in it. The coupled codes then will be used to study the PPI and, finally, to improve the overall interior ballistic simulation of ETC guns. In the hot plasma, the radiation by atoms and ions (the dissociation and ionization products of the capillary material or eventually of the propellant) dominates over molecules, and up to now we have focused on this hot radiation source. But in the next step, the absorption by the most important molecules (in the cold boundary layer of the plasma and the surrounding cold propellant gases) will be implemented as well. An adequate description of the radiation transport code, with all of its physical background, would go far beyond the scope of this report; only a summary of the basic theories with a focus on some important aspects is presented next.

---

## 2. Physical Background

---

In this section, the physics of plasma radiation is summarized; the reader is referred to some earlier work [5, 6], the final report of this Short-Term Analysis Service (STAS) contract [7], and the references therein for further details. The computation of the radiation transport equation (RTE) depends on frequency-dependent absorption coefficients  $\kappa_\nu$  and emission coefficients  $\varepsilon_\nu$ ,

which describe the interaction of the radiation field with matter (i.e., the atoms, ions, and molecules). The relation between absorption and emission are given under the assumption of a local thermodynamic equilibrium (LTE) by Kirchoff's law:

$$\varepsilon_\nu = \kappa_\nu I_\nu^0, \quad (1)$$

where  $I_\nu^0$  is the intensity of a black body radiator at frequency  $\nu$  and temperature  $T$ . Therefore, it is sufficient to calculate either the emission or, more commonly, the absorption coefficients, if LTE is assumed. These absorption coefficients depend on cross sections,  $\sigma_{ijk}$ , for line and continuum absorption and on the number densities,  $N_{ijk}$ , of species  $k$  in ionization stage  $j$  and excitation level  $i$ . Some aspects in the theoretical calculation of these quantities will be discussed in the following subsections.

## 2.1 Equation of State (EOS)

An essential difficulty in obtaining equations of state for plasmas arises from the fact that the Coulomb potential of the ionized species give rise to an infinite number of energy levels. The high levels have large radii, which eventually become larger than the mean interparticle distances in the plasma. Furthermore, the required partition functions then become infinite. For these reasons, some cut-off procedures have been introduced in the past. The most common ones are based on the Debye or Debye-Hueckel Theory, which leads to a reduction of the ionization potential. At higher pressures, when the Debye Theory is not valid anymore, often the Ion-Sphere Model is introduced—all levels with a radius larger than the mean interparticle distance cannot exist in this theory. Theories which assume a fixed cut off at any excited quantum level often lead to useful results when calculating thermodynamic properties of hot gases, but they lead to some unphysical behavior when dealing with optical quantities, i.e., the sharp edges of photo-ionization cross sections at the threshold of the photo-ionization energy, which never have been observed in experimental measurements. Within the framework of the OPACITY Project [8], an international collaboration concerned with the calculation of opacities of stellar envelopes, Hummer and Mihalas [9] introduced an occupation probability formalism for the calculation of the internal partition function:

$$Z_{jk}^I \equiv \sum_i w_{ijk} g_{ijk} e^{-E_{ijk}/k_B T}. \quad (2)$$

Here,  $g_{ijk}$  is the statistical weight,  $w_{ijk}$  is the occupation probability,  $E_{ijk}$  is the energy of the level,  $k_B$  is the Boltzmann constant, and  $T$  is the temperature. The  $w_{ijk}$  go to zero for higher states, which ensures that the sum in equation 2 is convergent. Interaction with charged and neutral surrounding particles is taken into account. The perturbations by neutral species are based on an excluded volume (hard-sphere) treatment (first term on the right of equation 3) and perturbations by charged particles are calculated from a fit to a quantum mechanical Stark ionization theory (using a first-order perturbation theory and a Holtzmark distribution for the ion microfield [second term of equation 3]):

$$\ln w_{ijk} = -\left(\frac{4\pi}{3}\right) \left\{ \sum_{\nu} N_{\nu} (r_{ijk} + r_{1\nu})^3 + 16 \left[ \frac{(Z_{jk} + 1)e_0^2}{\chi_{ijk} k_{ijk}^{1/2}} \right]^3 \sum_{k',j'} N_{j'k'} Z_{j'k'}^{3/2} \right\}. \quad (3)$$

The index  $\nu$  runs over all neutral species only;  $r_{1\nu}$  is the ground state radius of the neutral perturber, and  $r_{ijk}$  is the radius associated with state  $i$  of species  $k$  in ionization stage  $j$  of the perturbed atom.  $Z_{jk}$  is the net charge ( $Z_{jk} = 0$  for neutrals),  $\chi_{ijk}$  is the ionization energy, and  $k_{ijk}$  is a quantum mechanical correction and the sum in term two runs over all charged particles excluding electron. By use of this occupation probability formalism, the number densities in each excitation state are then given by a modified Boltzmann equation:

$$N_{ijk} = N_{jk} g_{ijk} w_{ijk} e^{-E_{ijk}/k_B T} / Z_{jk}^I. \quad (4)$$

A comparison of the simulated emission spectrum of the hydrogen Balmer series to experimental results by Wiese et al. [10] will be shown later. It can be seen that the occupation formalism leads to dissolution of the higher lines of the spectral series, resulting in a smooth transition to the continuum and an excellent agreement with the experimental measurements.

For the calculation of the ionization equilibrium number densities, an extended version of the NASA-Lewis code [11, 12] is used, which has been modified to simulate hot gases and plasmas [13, 14] (extension to high temperatures, including a collision cross-section database for calculation of transport coefficients and using a virial-type EOS for high-pressure conditions). The code is based on the free-energy minimization procedure in the ‘‘chemical picture,’’ assuming an LTE. In the future, the particle number densities might be estimated with Nusca’s NSRG2 code [15], including Anderson’s rate equation submodule [16]. Figure 1 shows calculated number densities for polyethylene plasmas at temperature and pressure conditions that typically occur in current ARL plasma jet experiments [4].

## 2.2 Absorption Coefficients

The cross section for line absorption (bound-bound) is given by

$$\sigma_{i,i'}^{bb}(\nu) = \frac{\pi e^2}{m_e c} \cdot f_{i,i'} I_{i,i'}(\nu), \quad (5)$$

with the charge of an electron  $e$ , its mass  $m_e$ , and the velocity of light  $c$ ;  $f_{i,i'}$  is the oscillator strength for a transition  $i \rightarrow i'$ , and  $I_{i,i'}$  is the profile of the line.

Line profiles for atoms and ions in a plasma are determined by electron impacts and by ion microfields. Griem [17] has made extensive calculations for these processes, and Konjević et al. [18] have reviewed experimental data. It was found that the experimental data are in good agreement with calculations made using the methods of Griem. In the semi-empirical electron

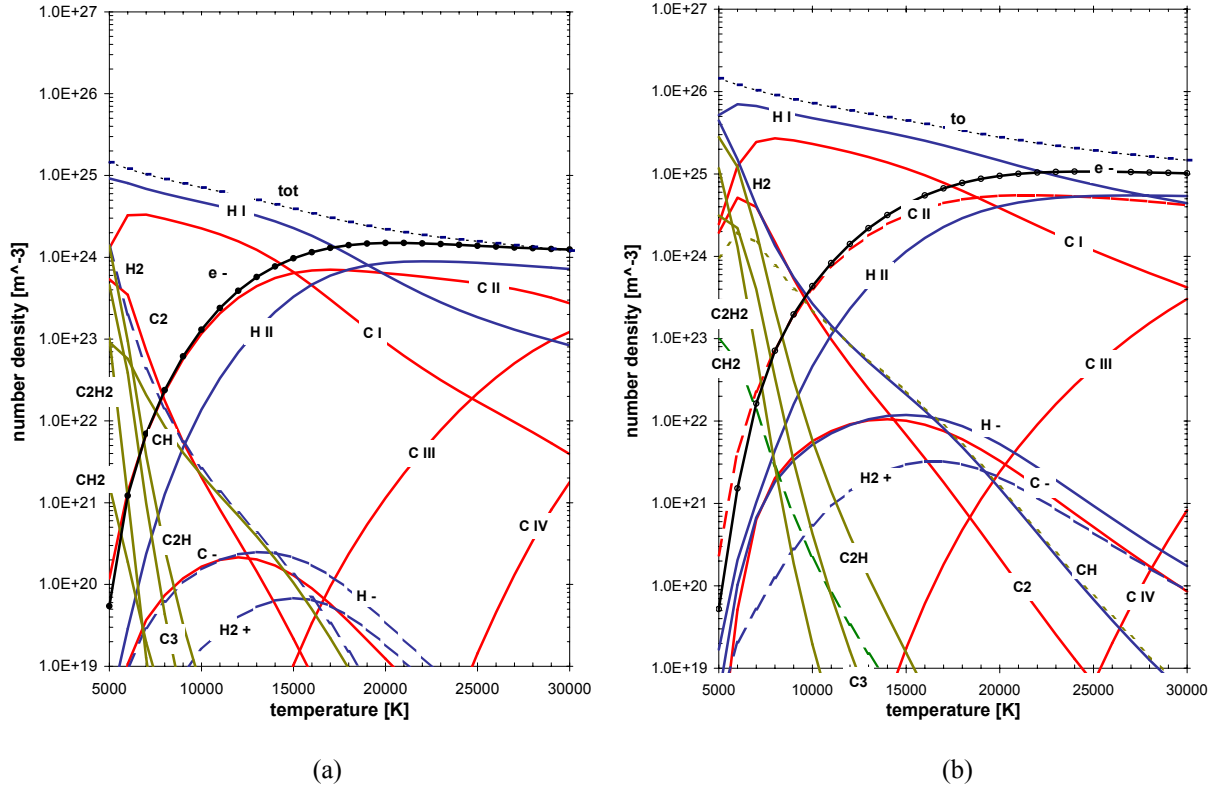


Figure 1. Calculated LTE number densities of a polyethylene ( $C_2H_4$ ) plasma at (a) 1 MPa and (b) 10 MPa.

impact approximation by Griem [17, 19] and Baranger [20], the full width of the line at half maximum (FWHM) is given by

$$\Gamma_S = 16 \left( \frac{\pi}{3} \right)^{3/2} \frac{h}{m_e a_0} n_e \left( \frac{Ry}{k_B T} \right)^{1/2} \left[ \sum_{i' \neq i} | \langle i' | r | i \rangle |^2 \bar{g}_i + \sum_{f' \neq f} | \langle f' | r | f \rangle |^2 \bar{g}_f \right]. \quad (6)$$

Here,  $Ry$  is the Rydberg energy,  $h$  is Planck's constant,  $a_0$  is Bohr's radius, and the matrix elements can be expressed as

$$| \langle i' | r | i \rangle |^2 = S(J', J) / g_i, \quad (7)$$

with the line strength  $S$  for a transition  $i \rightarrow i'$ ;  $g_i$  in equation 7 is the statistical weight of the ground level, and the sums running over all levels with an allowed transition to the state  $i$  ( $f$ ). The  $\bar{g}$  values in equation 6 are the so-called effective Gaunt factors [17] for the initial and final states

$$\bar{g}_i \equiv \bar{g}_i \left( \frac{3k_B T}{2|\Delta E_i|} \right). \quad (8)$$

The profile of the line in the case of electron impact broadening has a Lorentzian shape

$$I^L(\omega) = \frac{1}{\pi} \frac{(\Gamma_L/2)}{(\omega - \omega_0)^2 + (\Gamma_L/2)^2}, \quad (9)$$

and when Doppler broadening is also taken into account, the convolution of the two profiles is assumed to have a Voigt shape. For further details of the theory of line broadening, the reader is referred to the work of Griem and other standard literature.

For the calculation of line absorption coefficients, the oscillator strengths for all transitions have to be known. The oscillator strength for a transition  $i \rightarrow i'$  is

$$f_{i \rightarrow i'} = \frac{1}{3} \frac{(E_{i'} - E_i)}{g_i} S. \quad (10)$$

In all cases considered here, a single outer electron participates in the transition. Assuming an LS coupling scheme, the line strength may be written as [21]

$$S = l_{>} [J, J', L, L'] \begin{Bmatrix} L_c & l & L \\ 1 & l' & l' \end{Bmatrix} \begin{Bmatrix} L & S & J \\ J' & 1 & L' \end{Bmatrix} (R_{ni}^{n'l'})^2. \quad (11)$$

Here the first bracket  $[.]$  is shorthand for

$$[J, J', L, L'] = (2J+1)(2J'+1)(2L+1)(2L'+1),$$

and the  $\{.\}$  brackets refer to Wigner 6-j symbols [21], whose values can be evaluated analytically. The designations  $l$  ( $l'$ ) refer to the orbital angular momentum of the outer electron, with  $l_{>}$  being the greater of these;  $L$  ( $L'$ ) denotes the total orbital angular momentum,  $L_c$  being that of the core electrons; and  $J$  ( $J'$ ) denotes the total angular momentum of the state  $i$  ( $i'$ ). Finally, the square of the radial integral  $(R_{ni}^{n'l'})$  is calculated in the Coulomb approximation of Bates and Damgaard [22].

For isolated lines in non-hydrogenic systems, the broadening by ions is of secondary importance. Therefore, broadening by ions is not taken into account here, with the following exception: In the case of neutral atoms of carbon, nitrogen, and oxygen, Seaton [23] presented a fit formula that yields results within a factor of 2 of Griem's [19] published results. This formula is based on the previously described line strengths and is used for CI, NI, and OI. Stehlé [24] has published tables for Stark broadened hydrogen lines. Her calculation is based on the Model Microfield Method (MMM) for both the electronic and ionic broadenings and gives an accurate description of the line profile from the center to the wings. These data for the hydrogen Lyman, Balmer, and Paschen series are used up to electron number densities of  $10^{19} \text{ cm}^{-3}$ .

The photoionization cross sections are calculated in the classical theory by Kramers. This theory was developed for hydrogen and hydrogen-like species, which means that for the low-ionized plasmas in ETC applications the corresponding equations are only correct for hydrogen itself. Better agreement for multi-electron systems is obtained, especially for high excited states (which can be assumed to be hydrogen-like), by use of effective quantum numbers or the effective

nuclear charges, respectively. For the photoionization cross sections from the ground states of carbon, nitrogen, and oxygen published data of more detailed calculations have been adopted. In addition, so called Biberman or Biberman-Norman factors, which describe the difference of cross sections for multi-electron species to the hydrogen-like one, have been used for carbon, nitrogen, oxygen, and their first ionization stages. As will be shown in section 3, calculated cross sections are in good agreement to the published data, e.g., to NI cross sections given by Wilson and Nicolet [25].

### 2.3 Method of Partial Characteristics

The basis for quantitative studies of radiative energy transport is the radiation transport equation (RTE). Exact solution of this equation takes many hours of CPU time because thousands of absorption coefficients for the continuum and the spectral lines have to be considered for every iteration step when solving the energy balance equation. Simple tabulation of the absorption coefficients in the presence of spectral lines is also virtually impossible. Therefore, approximate but effective methods of integration of radiation characteristics are necessary. One integral method that gives values very close to the exact solution is the Method of Partial Characteristics (MPC) presented by Sevastyanenko [26, 27]. In this method, the complete description of the radiation field is possible by use of precalculated partial intensities

$$\Delta I(\xi, X) = \int_0^\infty I_\nu^0(T_\xi) k'_\nu(T_\xi, P_\xi) \exp\left(-\int_0^x k'_\nu(T_\eta, P_\eta) d\eta\right) d\nu. \quad (12)$$

Here,  $\Delta I(\xi, X)$  is the contribution to the intensity at point  $X$  at temperature  $T_X$  and pressure  $p_X$ , emitted at point  $\xi$  with its local conditions  $T_\xi$  and  $p_\xi$  and taken into account absorption along the path  $\overline{0X}$ .

The radiation intensity at point  $X$  then easily can be estimated by a simple integration along a ray  $\overline{0X}$ :

$$I(X) = \int_0^X \Delta I(\xi, X) d\xi, \quad (13)$$

and the radiation flux at  $X$  is obtained by integration over all directions

$$\vec{S}(X) = \iint_{4\pi} I(X) \vec{\Omega} d\Omega. \quad (14)$$

Using the MPC, it is possible to generate tables of radiation quantities for rapid calculations of radiation transfer in gas-dynamic simulations [5, 28]. A more detailed summary of the MPC can be found in an earlier paper [6] or in the original work of Sevastyanenko [26, 27].

## 2.4 Three-Dimensional (3-D) Radiation Transfer

The ARL NSRG2 CFD code [15] solves the two-dimensional (2-D)/axisymmetric and time-dependent Navier-Stokes equations by use of a finite-volume method. That means for a given grid cell, it balances the transfer of mass, momentum, and energy from and to all neighbor grid cells. For the radiation field, we have to know not only the contribution from the neighbor grid cells, but also the contribution from all cells having a line-of-sight to the cell of interest. For this reason, a quasi-3-D integration method has been developed, which integrates the partial radiation intensities of the whole 3-D volume for every grid point of the 2-D CFD grid, i.e., all grid points  $\xi'(r', \varphi, z')$  of the 3-D volume having a line-of-sight to a grid point  $X(r, z)$  of the 2-D CFD grid are taken into account. The necessary conditions at any point of the 3-D volume, e.g., the temperature, can easily be estimated from the 2-D grid, if the radial and longitudinal coordinates  $r'$  and  $z'$  of the point  $\xi'$  are known. A detailed description of this quasi-3-D integration submodule will be given elsewhere [7]. This 3-D integration submodule, together with some routines for the interpolation of radiation characteristics from the databases, are the only parts of the overall radiation code which will be integrated in the CFD code.

---

## 3. Validation

---

The final ARL plasma flow and PPI simulation code will contain highly sophisticated submodules like the radiation transport module, a module for solving the required rate equations, an ablation, and ignition module, etc. The validation of the coupled modules is a difficult part, for which reliable experimental data have to be available, too. A better way than to validate the overall program in a single step is to validate the different submodules as stand-alone programs first. In the case of the radiation part, the results of some comparisons to published theoretical and experimental data will be shown.

### 3.1 Atomic Data

About 150 calculated oscillator strengths and about 100 calculated line widths have been compared to the extensive compilation of the U.S. National Institute of Standards and Technology (NIST) [29] and the standard reference tables of Griem [17] for the atoms and ions of C, N, and O (for hydrogen the theories are exact). Almost all values are within a factor of 2 to the references, whereas most of them deviate only by a maximum of 20%. For example, Tables 1 and 2 show some results for the oscillator strengths of neutral carbon CI and the Stark broadening of single ionized carbon CII.

Table 1. Comparison of some calculated oscillator strengths of neutral carbon CI to data of Wiese et al. [29].

Transition $nl \rightarrow n'l'$	Multipl	$g_i - g_f$	$E_i$ ( $\text{cm}^{-1}$ )	$E_f$ ( $\text{cm}^{-1}$ )	$f_{if}$ (this work)	$f_{if}$ (Wiese et al. [29])
2p – 3s	$^3P - ^3P^o$	3 – 5	16.40	60393.14	6.615E! 02	5.88e! 02
		1 – 3	0.00	60352.63	1.592E! 01	1.40e! 01
		5 – 5	43.40	60393.14	1.191E! 01	1.04e! 01
		3 – 3	16.40	60352.63	3.981E! 02	3.56e! 02
		3 – 1	16.40	60333.43	5.316E! 02	4.71e! 02
		5 – 3	43.40	60352.63	3.982E! 02	3.56e! 02
2p – 3s	$^1S - ^1P^o$	1 – 3	21648.01	61981.82	1.251E! 01	9.40e! 02
3s – 4p	$^3P^o - ^3P$	1 – 3	60333.43	81325.76	5.247E! 03	3.44e! 03
		3 – 5	60352.63	81343.99	2.294E! 03	1.54e! 03
		3 – 3	60352.63	81325.76	1.298E! 03	8.04e! 04
		3 – 1	60352.63	81311.01	1.648E! 03	1.22e! 03
		5 – 5	60393.14	81343.99	4.041E! 03	2.72e! 03
		5 – 3	60393.14	81325.76	1.269E! 03	9.94e! 04
3s – 3p	$^3P^o - ^3D$	3 – 5	60352.63	69710.66	3.757E! 01	3.99e! 01
		1 – 3	60333.43	69689.48	5.004E! 01	5.34e! 01
		5 – 7	60393.14	69744.03	4.215E! 01	4.42e! 01
		3 – 3	60352.63	69689.48	1.250E! 01	1.29e! 01
		5 – 5	60393.14	69710.66	7.502E! 02	7.60e! 02
		5 – 3	60393.14	69689.48	4.990E! 03	4.95e! 03
3s – 4p	$^1P^o - ^1P$	3 – 3	61981.82	80562.85	5.006E! 03	8.08e! 03
3d – 6s	$^3D - ^3P^o$	3 – 5	69689.48	86369.60	1.886E! 04	1.93e! 04
		5 – 5	69710.66	86369.60	1.700E! 03	1.74e! 03
		3 – 3	69689.48	86331.63	2.829E! 03	2.89e! 03
		3 – 1	69689.48	86321.94	3.768E! 03	3.85e! 03
		7 – 5	69744.03	86369.60	6.820E! 03	6.93e! 03
		5 – 3	69710.66	86331.63	5.100E! 03	5.21e! 03

Note: Many thousands values for the atoms and ions of hydrogen, carbon, nitrogen, and oxygen are taken into account in the radiation transport code.

In Figure 2, a comparison of a calculated continuum spectrum for neutral nitrogen to results by Armstrong et al. (published by Wilson and Nicolet [25]) is shown. Good agreement is obtained and, whereas the spectrum of Armstrong shows the sharp edges at the photoionization thresholds, the present results using the occupation probability formalism are more physical.

To get good and reliable experimental data is often as difficult as it is to calculate them. Wiese et al. [10] published experimental data of emissivities of the hydrogen Balmer series, which have often been used for validation of theory and simulation. In Figure 3, current simulation results are compared to these measured data at two different temperatures and electron number densities. In addition to free-free Bremsstrahlung and bound-free recombination of HI, the photo attachment to the negative hydrogen is included in the simulation. Both theoretical and experimental emissivities are absolute, i.e., no scaling has been applied.

Table 2. Comparison of some calculated Stark broadened widths (FWHM) for single ionized carbon CII.

Transition $nl \rightarrow n'l'$	Multiplat	$\lambda$ (Å)	T $10^4$ (K)	$N_e$ $10^{16}$ ( $\text{cm}^{-3}$ )	$\gamma^a$ (Å)	$\gamma^b$ (Å)	$\gamma^c$ (Å)
2p – 3s	$^2P^o - ^2S$	858	10	10.0	6.699e! 3	6.889e! 3	1.650e! 2
			20	10.0	4.737e! 3	4.871e! 3	1.300e! 2
3s – 3p	$^2S - ^2P^o$	6580	10	10.0	8.324e! 1	8.371e! 1	1.192e+0
			20	10.0	5.886e! 1	5.919e! 1	1.038e+0
3s – 4p	$^2S - ^2P^o$	2174	20	10.0	2.130e! 1	2.267e! 1	2.960e! 1
3p – 3d	$^2P^o - ^2D$	7234	20	10.0	8.669e! 1	1.068e+0	1.198e+0
3p – 4s	$^2P - ^2S$	3920	20	10.0	8.604e! 1	6.492e! 1	9.600e! 1
3p – 4d	$^2P^o - ^2D$	2747	20	10.0	1.153e+0	1.392e+0	9.360e! 1
3d – 4p	$^2D - ^2P^o$	5890	20	10.0	1.667e+0	1.896e+0	2.180e+0
3d – 4f	$^2D - ^2F^o$	4267	20	10.0	1.259e+0	2.571e+0	1.690e+0
3d – 5p	$^2D - ^2P^o$	3361	20	10.0	1.999e+0	2.754e+0	1.836e+0
3d – 5f	$^2D - ^2F^o$	2993	10	10.0	3.567e+0	4.919e+0	4.560e+0
			20	10.0	3.060e+0	5.241e+0	3.840e+0

<sup>a</sup>Comparison made by method described in text.

<sup>b</sup>Comparison made by a simpler approximation for the matrix elements.

<sup>c</sup>Comparison made with values given by Griem [17] (core configuration is  $2s^2(^1S)$ ).

Note: Many thousands widths for the lines of atoms and ions of hydrogen, carbon, nitrogen, and oxygen are taken into account in the radiation transport code.

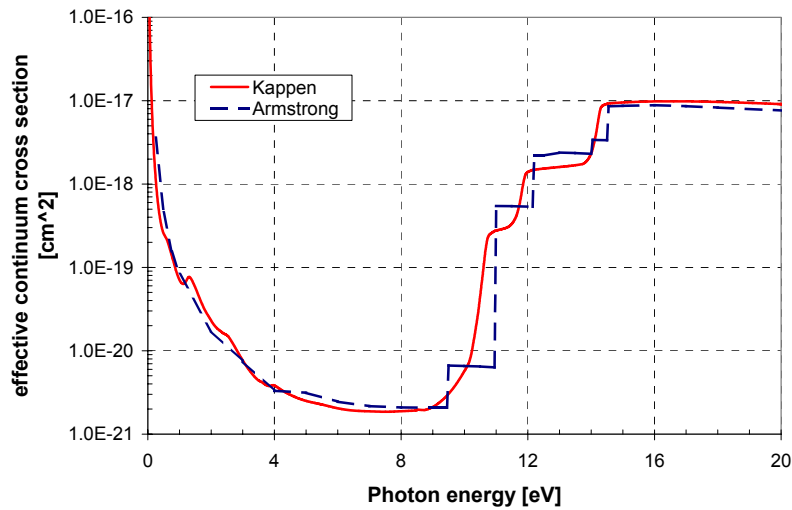


Figure 2. Comparison of calculated total effective continuum cross section for Ni at 15,000 K. The results of Armstrong et al. [30] have been published by Wilson and Nicolet [25].

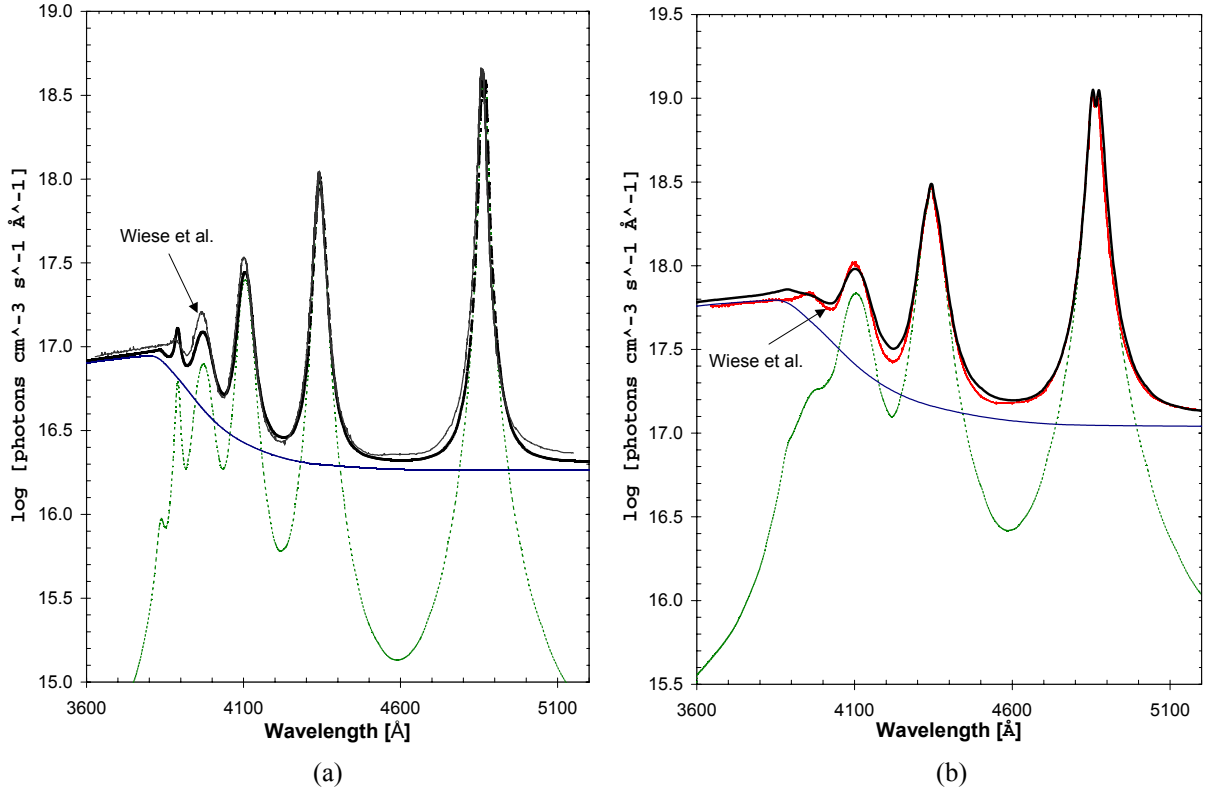


Figure 3. Emissivities of hydrogen (a)  $N_e = 2.9 \times 10^{16} \text{ cm}^{-3}$  and  $T = 10,850 \text{ K}$  and (b)  $N_e = 9.3 \times 10^{16} \text{ cm}^{-3}$  and  $T = 13,140 \text{ K}$ , compared to experimental data of Wiese et al. [10]. The thin lines are the contribution due to lines and the continuum. The smooth dissolution of the line into the continuum agrees very well with the measurements.

### 3.2 Net Emission Coefficients

To validate the integrated radiation characteristics stored as databases, net emission coefficients have been calculated and compared to published results. Lowke [31] has shown that the averaged radiation intensity of an isothermal cylinder with radius  $R$  is approximately the same as for an isothermal sphere. By using the simpler formula for the sphere, the net emission coefficient is given as

$$\varepsilon_N = \int_0^{\infty} I_{\nu}^0 k'_{\nu} \exp(-k'_{\nu} R) d\nu.$$

From equations 12 and 13 it can easily be seen that the net emission coefficient can be estimated from the radiation characteristics database if we use an isothermal temperature profile with  $T_x = T_{\xi}$  and radius  $X = R$ . In Figure 4, a comparison of net emission coefficients for high temperature air and  $\text{SF}_6^*$  is shown.

\* The calculations of  $\text{SF}_6$  have only been performed for validation purposes; there is no interest in this gas for ETC applications.

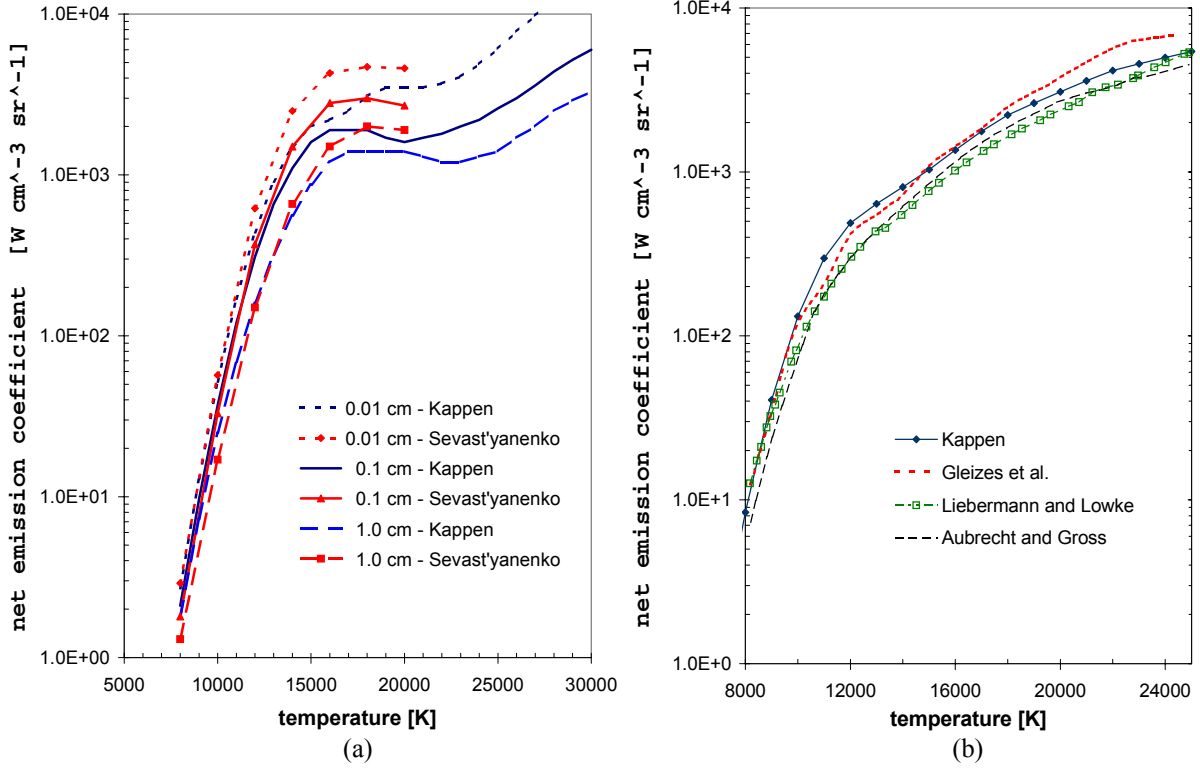


Figure 4. Net emission coefficients of (a) an isothermal air plasma at different radii and (b) an isothermal SF<sub>6</sub> plasma of radius 0.1 cm, compared to results of Sevastyanenko and Soloukhin [32], Gleizes et al. [33], Liebermann and Lowke [34], and Aubrecht and Gross [35]. All calculations have been performed for atmospheric pressure.

Current efforts are the validation of the 3-D model. First results indicate that it is working well, so in the next step of the STAS program an interface between the RT code and the CFD code will be set up and tested.

## 4. Radiation Transport in CFD Simulations

There are two aspects of radiation in ETC CFD simulation: first, the energy transfer by radiation in the hot plasma and gas, and second, the interaction of the radiation energy that is transmitted to the capillary wall or propellant. The current ARL CFD codes do not include the ohmic heating in the energy balance, i.e., the equation that is solved may be written as [15]

$$\frac{\partial(\rho e)}{\partial t} + \nabla \cdot (\rho \bar{v} e) + p \cdot \nabla \bar{v} + \nabla \bar{q} + \nabla \bar{S} = 0, \quad (15)$$

with the density  $\rho$ , the velocity  $\bar{v}$ , the energy  $e$ , the pressure  $p$ , and the thermal heat flux  $\bar{q}$ . The divergence of the radiation flux  $\bar{S}$  will be calculated directly by use of the MPC without numerical differentiation. From the inner hot core of the plasma to the outer cold gas zone, this  $\nabla \bar{S}$  term will change its sign: whereas the radiation is mainly responsible for energy losses in

the hot core, a lot of radiation energy will be reabsorbed at the cold boundary and the surrounding gas, leading to a temperature increase in this regions. Regarding the interface, only the 3-D integration submodule together with some interpolation routines and the MPC databases will be coupled to the CFD code. In every iteration and time step when the energy balance is solved, the CFD code will call the radiation submodule with the actual pressure and temperature profile (for all grid points), and the divergence of the radiation flux will be given back.

When taking into account material ablation in the capillary and/or ignition of a propellant, in addition to the  $\nabla \bar{S}$  values the radiation energy flux at the wall (or grains) is required. Calling the RT code for a second time, which in that case will use a different integration algorithm [6], this can be done. The resulting radiation energy will then be used for PPI studies, in new pyrolysis laws and/or ablation modules in the CFD simulation. Regarding propellants, which may be transparent for parts of the electromagnetic spectrum, one might be interested in the energy transfer within different frequency bands. Using the presented radiation transport code, either the total energy transfer from the vacuum ultraviolet (VUV) to the infrared (IR) or by radiation of some frequency bands of special interest can be calculated.

---

## 5. Summary

---

A new radiation transport code has been described, which will be used in the ARL NSRG2 code for the plasma-propellant interaction simulation. With the implemented method of partial characteristics it is possible to precalculate databases, which allow one to calculate the energy transfer by radiation iteratively at the same time when solving the balance equations of mass, momentum, and energy in any CFD code in an acceptable CPU time. Some efforts for the validation of the program have been presented, and it has been shown that the current version of the code yields results, which are in very good agreement to published theoretical as well experimental data. In addition, a 3-D integration method has been implemented, which allows one to use the code for calculations in any cylinder-symmetrical volume (the precalculated partial intensities stored in the databases are independent of the geometry); the validation of this part is almost finished. In a next step, absorption of the most important molecules will be added to the code and current efforts are the coupling of the RT code to the ARL NSRG2 code. The focus of the current activities is on plasmas containing molecules, atoms, and ions of hydrogen, carbon, nitrogen, and oxygen, but the program is in no way limited to this. Finally, the performance of some laboratory experiments is underway to validate the CFD code with incorporated radiation simulation.

Until now, the radiation transport code consists of more than 40 subroutines and 6 input databases/files for the energy level, quantum numbers, etc. Finally, a graphical user interface (GUI) has been developed, which allows one to use the code without extensive knowledge of quantum mechanics and plasma physics.

---

## 6. References

---

1. White, K. J., G. L. Katulka, and S. Driesen. "Electrothermal-Chemical Plasma Interaction With Propellants." *32nd JANNAF Combustion Subcommittee Meeting*, CPIA Publication 631, 1995.
2. Koleczko A., W. Erhardt, S. Kelzenberg, and N. Eisenreich. "Plasma Ignition and Combustion." 32nd International Annual Conference of ICT, 2001.
3. Koleczko, A., and N. Eisenreich. Personal communications. Fraunhofer Institute for Chemical Technologies, Pfinztal, Germany, 1999.
4. Beyer, R. A. "Small Scale Experiments in Plasma Propellant Interactions." *Proceedings of the 37th JANNAF Combustion Subcommittee Meeting*, CPIA Publication 701, vol. 1, p. 137, 2000.
5. Kappen, K., and U. H. Bauder. "Calculation of Plasma Radiation Transport for Description of Propellant Ignition and Simulation of Interior Ballistics in ETC Guns." *IEEE Transactions on Magnetics*, vol. 1, 2001.
6. Kappen, K., and U. H. Bauder. "Simulation of Plasma Radiation in Electrothermal-Chemical Accelerators." *IEEE Transactions on Magnetics*, vol. 35, no. 1, 1999.
7. Kappen, K. STAS Contract DAAH04-96-C-0086. Unpublished data.
8. Seaton, M. J. "Opacities for Stellar Envelopes." *Monthly Notices of the Royal Astronomical Society*, vol. 266, p. 805, 1994.
9. Hummer, D. G., and D. Mihalas. "An Occupation Probability Formalism for the Truncation of the Internal Partition Function." *The Astrophysical Journal*, vol. 331, p. 794, 1988.
10. Wiese, W. L., D. E. Kelleher, and D. R. Paquette. "Detailed Study of the Stark Broadening of Balmer Lines in High-Density Plasma." *Physical Review A*, vol. 6, no. 3, p. 1132, 1972.
11. Gondon, S., and B. J. McBride. "Computer Program for the Calculation of Complex Chemical Equilibrium Compositions, Rocket Performance, Incident and Reflected Shocks, and Chapman-Jourguet Detonations." NASA-SP-273, NASA-Lewis Research Center, Cleveland, OH, 1971.
12. Svehla, R. A., and B. J. McBride. "Fortran IV Computer Program for the Calculation of Thermodynamic and Transport Properties of Complex Chemical Systems." NASA-TN-D-7056, NASA-Lewis Research Center, Cleveland, OH, 1973.

13. Kovitya, P. "Theoretical Determination of Material Functions of Plasmas Formed of Ablated PTFE, Aluminium, PVC, and Perspex for Temperature Range of 5000 to 30000 K." CSIRO Division of Applied Physics TM No. 3, Lindfield, New South Wales, Australia, 1982.
14. Kappen, K. "Berechnung der Materialfunktionen von Hochdruckplasmen am Beispiel von Methanol." Diploma thesis, Technical University Munich, 1995.
15. Nusca, M. J., M. J. McQuaid, and W. R. Anderson. "Development and Validation of a Multi-Species Reacting Flow Model for the Plasma Jet Generated by an ETC Igniter." *Proceedings of the 37th JANNAF Combustion Subcommittee Meeting*, CPIA Publication 701, p. 1, 2000.
16. Nusca, M. J., and W. R. Anderson. "CFD Model of the Plasma Efflux Generated by an ETC Igniter: Characterization of Propellant Surface Conditions." *Proceedings of the 38th JANNAF Combustion Subcommittee Meeting*, 2002.
17. Griem, H. R. *Spectral Line Broadening by Plasmas*. New York: Academic Press, 1974.
18. Konjević, N., M. S. Dimitrijević, and W. L. Wiese. *Journal of Physical and Chemical Reference Data*. Vol. 13, p. 619, 1984.
19. Griem, H. R. "Semiempirical Formulas for the Electron-Impact Widths and Shifts of Isolated Ion Lines in Plasmas." *Physical Review*, vol. 165, no. 1, p. 258, 1968.
20. Baranger, M. *Physical Review*. Vol. 111, p. 494, 1958.
21. Cowan, R. D. *The Theory of Atomic Structure and Spectra*. Berkeley: University of California Press, 1981.
22. Bates, D. R., and A. Damgaard. *Philosophical Transactions of the Royal Society of London, Series A: Mathematical and Physical Sciences*, p. 242, 1949.
23. Seaton, M. J. "Atomic Data for Opacity Calculations: XII. Line-Profile Parameter for Neutral Atoms of He, C, N, and O." *Journal of Physics B: Atomic Molecular and Optical Physics*, vol. 22, p. 3603, 1989.
24. Stehlé, C., and R. Hutcheon. "Extensive Tabulations of Stark Broadened Hydrogen Line Profiles." *Astronomy and Astrophysics Supplement*, vol. 144, p. 93, 1999.
25. Wilson, K. H., and W. E. Nicolet. "Spectral Absorption Coefficients of Carbon, Nitrogen, and Oxygen Atoms." *Journal of Quantitative Spectroscopy & Radiative Transfer*, vol. 7, p. 891, 1967.
26. Sevastyanenko, V. G. "Radiation Transfer in a Real Spectrum: Integration Over Frequency." *Inzhenerno-fizicheskii Zhurnal*, vol. 36, no. 2, 1979.

27. Sevastyanenko, V. G. "Radiation Transfer in a Real Spectrum: Integration With Respect to Frequency and Angles." *Inzhenerno-fizicheskii Zhurnal*, vol. 38, no. 2, 1980.
28. Gruber, K., K. Kappen, A. Voronov, and H. Haak. "Radiation Absorption of Propellant Gas." *IEEE Transactions on Magnetics*, vol. 1, 2001.
29. Wiese, W. L., J. R. Fuhr, and T. M. Deters. "Atomic Transition Probabilities of Carbon, Nitrogen, and Oxygen—A Critical Data Compilation." *Journal of Physical and Chemical Reference Data*, monograph no. 7, 1996.
30. Armstrong, B. H., R. R. Johnston, and P. S. Kelly. "Opacity of High Temperature Air." Lockheed Missiles & Space Co. Report No. 8-04-64-2, 1964.
31. Lowke, J. J. "Predictions of Arc Temperature Profiles Using Approximate Emission Coefficients for Radiation Losses." *Journal of Quantitative Spectroscopy & Radiative Transfer*, vol. 14, p. 111, 1973.
32. Sevastyanenko, V. G., and R. I. Soloukhin. *Handbook of Radiative Heat Transfer in High-Temperature Gases*. New York: Hemisphere Publishing Corporation, 1987.
33. Gleizes, A., B. Rahmani, J. J. Gonzales, and B. Liani. *Journal of Physics D: Applied Physics*. Vol. 24, p. 1300, 1991.
34. Liebermann, R. W., and J. J. Lowke. *Journal of Quantitative Spectroscopy & Radiative Transfer*. Vol. 16, p. 253, 1976.
35. Aubrecht, V., and B. Gross. "Net Emission Coefficient of Radiation in SF<sub>6</sub> Arc Plasmas." *Journal of Physics D: Applied Physics*, vol. 27, p. 95, 1994.

INTENTIONALLY LEFT BLANK.

REPORT DOCUMENTATION PAGE			Form Approved OMB No. 0704-0188
Public reporting burden for this collection of information is estimated to average 1 hour per response, including the time for reviewing instructions, searching existing data sources, gathering and maintaining the data needed, and completing and reviewing the collection of information. Send comments regarding this burden estimate or any other aspect of this collection of information, including suggestions for reducing this burden, to Washington Headquarters Services, Directorate for Information Operations and Reports, 1215 Jefferson Davis Highway, Suite 1204, Arlington, VA 22202-4302, and to the Office of Management and Budget, Paperwork Reduction Project(0704-0188), Washington, DC 20503.			
1. AGENCY USE ONLY (Leave blank)	2. REPORT DATE September 2002	3. REPORT TYPE AND DATES COVERED Interim Report, June 2001 – March 2002	
4. TITLE AND SUBTITLE Radiation Transfer Modeling in Electrothermal Chemical (ETC) Ignition			5. FUNDING NUMBERS C: DAAH04-96-C-0086, TCN 01033, D.O. 0699
6. AUTHOR(S) Klaus Kappen			
7. PERFORMING ORGANIZATION NAME(S) AND ADDRESS(ES) Esterwagnerstraße 19 A 85635 Höhenkirchen GERMANY			8. PERFORMING ORGANIZATION REPORT NUMBER
9. SPONSORING/MONITORING AGENCY NAME(S) AND ADDRESS(ES) U.S. Army Research Laboratory ATTN: AMSRL-WM-BD Aberdeen Proving Ground, MD 21005-5066			10. SPONSORING/MONITORING AGENCY REPORT NUMBER ARL-CR-506
11. SUPPLEMENTARY NOTES The author is a Guest Researcher at ARL.			
12a. DISTRIBUTION/AVAILABILITY STATEMENT Approved for public release; distribution is unlimited.			12b. DISTRIBUTION CODE
13. ABSTRACT (Maximum 200 words) The use of plasma ignition for high-performance guns has been pursued at several levels. As part of the program at the U.S. Army Research Laboratory (ARL), we are attempting to define the role of the broadband electromagnetic radiation that is a key energy component of the plasma discharge. In particular, this effort is developing a radiation transfer model that will be incorporated into the computational fluid dynamics (CFD) model of plasma ignition. This effort will allow more physically realistic characterization of the energy transfer in the plasma and its interaction with the propellant in the models.  This report summarizes the physical background of the radiation transport, and the validation of the different submodules by use of published data will be presented. Current efforts include the coupling of the radiation model to the ARL NSRG2 code for the plasma-propellant interaction simulation. Furthermore, a series of laboratory experiments will be performed to validate the CFD code with the incorporated radiation transport submodel.			
14. SUBJECT TERMS plasma, propellant, ignition, radiation			15. NUMBER OF PAGES
			16. PRICE CODE
17. SECURITY CLASSIFICATION OF REPORT UNCLASSIFIED	18. SECURITY CLASSIFICATION OF THIS PAGE UNCLASSIFIED	19. SECURITY CLASSIFICATION OF ABSTRACT UNCLASSIFIED	20. LIMITATION OF ABSTRACT UL

NSN 7540-01-280-5500

17

Standard Form 298 (Rev. 2-89)  
Prescribed by ANSI Std. Z39-18 298-102

INTENTIONALLY LEFT BLANK.

<u>NO. OF COPIES</u>	<u>ORGANIZATION</u>	<u>NO. OF COPIES</u>	<u>ORGANIZATION</u>
2	DEFENSE TECHNICAL INFORMATION CENTER DTIC OCA 8725 JOHN J KINGMAN RD STE 0944 FT BELVOIR VA 22060-6218		<u>ABERDEEN PROVING GROUND</u>
		2	DIR USARL AMSRL CI LP (BLDG 305)
1	HQDA DAMO FDT 400 ARMY PENTAGON WASHINGTON DC 20310-0460		
1	COMMANDING GENERAL US ARMY MATERIEL CMD AMCRDA TF 5001 EISENHOWER AVE ALEXANDRIA VA 22333-0001		
1	INST FOR ADVNCD TCHNLGY THE UNIV OF TEXAS AT AUSTIN 3925 W BRAKER LN STE 400 AUSTIN TX 78759-5316		
1	US MILITARY ACADEMY MATH SCI CTR EXCELLENCE MADN MATH THAYER HALL WEST POINT NY 10996-1786		
1	DIRECTOR US ARMY RESEARCH LAB AMSRL D DR D SMITH 2800 POWDER MILL RD ADELPHI MD 20783-1197		
1	DIRECTOR US ARMY RESEARCH LAB AMSRL CI AI R 2800 POWDER MILL RD ADELPHI MD 20783-1197		
3	DIRECTOR US ARMY RESEARCH LAB AMSRL CI LL 2800 POWDER MILL RD ADELPHI MD 20783-1197		
3	DIRECTOR US ARMY RESEARCH LAB AMSRL CI IS T 2800 POWDER MILL RD ADELPHI MD 20783-1197		

NO. OF  
COPIES    ORGANIZATION

ABERDEEN PROVING GROUND

28    DIR USARL  
      AMSRL WM BD  
      W R ANDERSON  
      R A BEYER  
      A L BRANT  
      S W BUNTE  
      C F CHABALOWSKI  
      L M CHANG  
      T P COFFEE  
      J COLBURN  
      P J CONROY  
      R A FIFER  
      B E FORCH  
      B E HOMAN  
      S L HOWARD  
      P J KASTE  
      A J KOTLAR  
      C LEVERITT  
      K L MCNESBY  
      M MCQUAID  
      M S MILLER  
      A W MIZIOLEK  
      J B MORRIS  
      J A NEWBERRY  
      M J NUSCA  
      R A PESCE-RODRIGUEZ  
      G P REEVES  
      B M RICE  
      R C SAUSA  
      A W WILLIAMS

<u>NO. OF COPIES</u>	<u>ORGANIZATION</u>
1	SAIC FSU C C HSIAO 10260 CAMPUS POINT DR SAN DIEGO CA 92121
2	UDLP ARMAMENT SYSTEMS DIV W DICK R JOHNSON 4800 E RIVER ROAD MINNEAPOLIS MN 55421-1498
1	US ARMY RSRCH OFFICE D MANN PO BOX 12211 4300 S MIAMI BLVD RESEARCH TRIANGLE PARK NC 27709-2211
2	PENN STATE UNIV S THYNELL T LITZINGER 111 RESEARCH BUILDING E UNIVERSITY PARK PA 16802
1	UNIV OF TEXAS DEPT OF AEROSPACE ENGRG AND ENGRG MECHS P VARGHESE AUSTIN TX 78712-1085
1	NORTH CAROLINA STATE UNIV DEPT OF NUCLEAR ENGRG M BOURBAM 2109 BURLINGTON ENGRG LABS RALEIGH NC 27695-7907

NO. OF  
COPIES    ORGANIZATION

3    K KAPPEN  
ESTERWAGNERSTRASSE 19 A  
85635 HÖHENKIRCHEN  
GERMANY